

# Three-dimensional arterial spin labeling imaging and dynamic susceptibility contrast perfusion-weighted imaging value in diagnosing glioma grade prior to surgery

HONG MA<sup>1,2</sup>, ZIZHENG WANG<sup>1</sup>, KAI XU<sup>2</sup>, ZEFENG SHAO<sup>1</sup>, CHUN YANG<sup>2</sup>,  
PENG XU<sup>2</sup>, XIAOHUA LIU<sup>2</sup>, CHUNFENG HU<sup>2</sup>, XIN LU<sup>2</sup> and YUTAO RONG<sup>2</sup>

<sup>1</sup>Department of Nuclear Medicine, Nanjing First Hospital, Nanjing Medical University, Nanjing, Jiangsu 210006;

<sup>2</sup>Department of Radiology, The Affiliated Hospital of Xuzhou Medical University, Xuzhou, Jiangsu 221002, P.R. China

Received April 18, 2016; Accepted January 6, 2017

DOI: 10.3892/etm.2017.4370

**Abstract.** The current study aimed to investigate whole-brain three-dimensional arterial spin labeling imaging (3D ASL) and dynamic susceptibility contrast perfusion-weighted imaging (DSC-PWI), in regards to their diagnostic value of preoperative glioma grade. The parameter values obtained after correction will be correlated with the diagnostic value of 3D ASL and DSC-PWI perfusion. In the current study, 50 patients with gliomas confirmed by pathology were used, including 27 low-grade gliomas (LGGs) and 23 high-grade gliomas (HGGs). Prior to surgery all patients underwent 3 Tesla magnetic resonance imaging (MRI), 3D ASL, DSC-PWI and conventional enhanced MRI scans to obtain original 3D ASL and DSC-PWI images, and the tumor regions with the most obvious parenchyma perfusion and contralateral normal white matter were selected. In these areas, the ASL-relative cerebral blood flow (ASL-rCBF), DSC-relative cerebral blood flow (DSC-rCBF) and DSC-relative cerebral blood volume (DSC-rCBV) parameter values were then obtained after correction for individual differences. The results of the present study show that ASL-CBF, DSC-CBF, DSC-CBV values and ASL-rCBF, DSC-rCBF, DSC-rCBV values increased as the grade of the glioma being imaged increased, and there was a marked difference between the HGGs and the LGGs. ASL-rCBF was significantly positively correlated with DSC-rCBF ( $r=0.580$ ,  $P<0.01$ ). In addition, ASL-rCBF was significantly positively correlated with DSC-rCBV ( $r=0.431$ ,  $P<0.01$ ). Receiver operating characteristic (ROC) curves were

applied to compare the two perfusion parameters of DSC-PWI and 3D ASL in the diagnosis of glioma grade. ASL-rCBF had the highest area value under the ROC curve (0.836). The areas under the ROC curve of DSC-rCBF and DSC-rCBV were analyzed using the Z test, but the difference was not statistically significant. When ASL-rCBF, DSC-rCBF and DSC-rCBV were cutoff at 2.24, 1.85 and 1.68, the sensitivity of HGG diagnosis was 83.2, 91.3 and 91.3%, and the specificity was 77.7, 63.9 and 66.7%, respectively.

## Introduction

Glioma is the most common type of central nervous system tumor, according to the World Health Organization (WHO) (1). Glioma is divided into four grades; grades I and II are low level tumors, and grades III and IV are high level tumors (1,2). There are great differences in clinical treatment and prognosis between the different grades of gliomas, and preoperative identification of gliomas has important clinical significance (3). Conventional MRI image enhancement is the most common method used to determine between a benign and malignant glioma. It is typically considered that high-grade gliomas are notably enhanced by conventional magnetic resonance enhancement, while low-grade gliomas are not enhanced. However, in recent years this view has been questioned. In principle, the strengthening of magnetic resonance imaging (MRI) enhancement reflects tumor disruption of the blood-brain barrier (BBB), enhanced when the contrast agent used enters into the extravascular tissue space (4,5). However, the most obviously enhanced region does not reflect the region of the tumor with the highest degree of malignancy and regions of angiogenesis will not necessarily be enhanced. Despite invasive tumor growth along vascular access to white matter tracts, BBB are likely to remain intact, making imaging deviate from the actual pathology. Conventional MRI is not capable of providing details of the fine structure of the tumor microvessel density or angiogenesis information (6). So, there is a requirement for new imaging technologies that can provide this information.

Angiogenesis and tumor cell constitution are the primary indicators of the pathological grade of glioma (7). The capillary network can provide nutrients needed for growth of

---

*Correspondence to:* Dr Zizheng Wang, Department of Nuclear Medicine, Nanjing First Hospital, Nanjing Medical University, 68 Chang Le Road, Nanjing, Jiangsu 210006, P.R. China  
E-mail: zzwang136@aliyun.com

**Key words:** magnetic resonance imaging, three-dimensional arterial spin labeling, dynamic susceptibility contrast perfusion-weighted imaging, glioma

tumor cells and a way for the tumor to metastasize, such that angiogenesis factor production and tumor growth are inter-related. Previously, it was reported that dynamic susceptibility contrast perfusion-weighted imaging (DSC-PWI) of cerebral blood volume (CBV) and cerebral blood flow (CBF) is able to describe the blood supply of brain tumors quantitatively (8). An endogenous tracer is used in three-dimensional arterial spin labeling (3D-ASL) to evaluate tissue perfusion and should better reflect perfusion compared with MRI using a contrast agent. However, it is unclear whether or not ASL-CBF can reflect tumor angiogenesis, whether ASL-CBF is correlated with DSC-CBV and DSC-CBF, and whether ASL-CBF can more accurately evaluate the glioma grade compared with DSC-CBV and DSC-CBF.

The current study was designed to identify the relative values of ASL-CBF, DSC-CBF, DSC-CBV obtained from 3D ASL and DSC-PWI, the two perfusion weighted imaging technologies, to analyze the perfusion status in different grades of glioma, to explore their value in the preoperative grading of gliomas in patients and compare their accuracy in identifying the pathological grading.

## Materials and methods

*Patient selection and characteristics.* All patients were from The Affiliated Hospital of Xuzhou Medical University (Xuzhou, China). The present study was performed between December 2014 and October 2015. Patients with computerized tomography (CT) or MRI confirmed tumor lesions of the brain were selected for the study. Prior to MRI examination none of the patients were treated with chemotherapy, radiotherapy or surgery. MRI was conducted <1 week before surgery. A total of 72 cases of brain tumors, suspected to be glioma, were enrolled, with 22 excluded on the basis of motion artifacts (n=4), hemorrhage (n=6), not undergoing surgery or pathological confirmation that their tumor was not a glioma (n=12). Based on the pathology, the imaging data of 50 cases of patients with glioma were used in the present study. Following the WHO classification criteria 2007 (1), the gliomas cases were classified as low-grade (grades I and II, n=27) or high-grade (grades III and IV, n=23). In total there were 26 males and 24 females, aged between 14 and 84 years old (mean, 45.6 years). The primary clinical symptoms of the patients in the study included headache, dizziness, nausea, vomiting, seizures, decreased vision and language barriers.

*MRI examination.* All patients were imaged from the base to the top of the head using a 3.0 T superconducting MRI scanner (Discovery MR750 w 3.0T; GE Healthcare, Piscataway, NJ, USA). The gradient switching rate used was 120 mT/m/ms, with a gradient field intensity of 33 mT/m, using a 16-channel phased-array coil.

MRI scans consisted of conventional MRI (T2-weighted imaging, T1-weighted imaging, T2 fluid-attenuated inversion recovery, diffusion-weighted imaging and a pure axial scan of T2WI), 3D ASL, the use of a contrast agent for DSC-PWI and contrast enhanced T1WI (transverse, coronal, sagittal plane and a pure axial scan). Imaging was obtained with the parameters described in Table I. Perfusion was determined subjectively by the authors.

DSC-PWI was performed using a gradient recalled echo-echo planar imaging (GRE-EPI) sequence during the administration of 0.2 mol/kg of gadopentetic acid dimeglumine salt injection (Magnevist; Bayer Healthcare Pharmaceuticals, Berlin, Germany) at a rate of 3 ml/s. This was followed by a bolus injection of 20 ml saline. The DSC-PWI was performed using the same section orientations as those for conventional MRI.

*Image analysis.* Imaging data was automatically delivered to an AW4.6 workstation (Advantage for Windows; GE Healthcare) and analyzed using Functool v.9.4.05 analysis software (GE Healthcare). The conventional pure axial T2WI or pure axial enhanced T1WI MRI images and 3D-ASL or DSC-PWI perfusion images were fused, with the conventional image positioning. The region of interest (ROI) of the largest area of solid tumor perfusion was selected according to the color gradation of ASL or DSC-PWI perfusion pseudo color map (avoiding the sac, hemorrhage, large blood vessels and artifact-obvious area) and covered an area of 50-60 mm<sup>2</sup>. The contralateral normal ROI was selected by using the mirror image of the tumor ROI. ASL-CBF, DSC-CBF and DSC-CBV data of each ROI were measured three times and an average was calculated by two experienced neural radiologists.

*Analysis of pathological specimens.* All the specimens obtained by surgery were embedded in a paraffin block, cut into 3- $\mu$ m thick serial slices and examined by routine hematoxylin and eosin staining and immunohistochemical staining for glial fibrillary acidic protein (M-0262), Ki67 (M-0350), O-6-methylguanine-DNA methyltransferase (M-0382), P53 (M-0430), S100 (M-0466), Syn (M-0482; all Shanghai LongIsland Biotec. Co., Ltd., Shanghai, China) and isocitrate dehydrogenase 1 (ZM-0447; Beijing Zhongshan Golden Bridge Biotechnology Co., Ltd., Beijing, China) with fully automatic immunohistochemical staining apparatus (BenchMark XT; Roche Diagnostics, Basel, Switzerland). All antibodies were used at the dilutions provided in the respective antibody kits. Pathological sections were analyzed by two experienced neuropathology specialists. Based on the histological typing of the tumor cells, including factors such as atypical nuclei, tissue necrosis and the results of immunohistochemistry for Ki67, tumors were classified into low-grade gliomas (LGG; grade I, G1; grade II, GII) and high-grade gliomas (HGG; grade III, G3; grade IV, G4) according to the WHO criteria (2007).

*Statistical analysis.* Data analysis was performed using SPSS software (version 16.0; SPSS, Inc., Chicago, IL, USA). All the values were tested for consistency using the correlation coefficient for each parameter following agreement between the two surveyors. Data were divided into two groups, a LGG and HGG group, based on the pathological stage. Then, normality and homogeneity of variance of the measured parameters was determined using exploratory analysis (Explore tool; SPSS, Inc.). Conformance to the normal distribution of quantitative data is shown as the mean  $\pm$  standard deviation, or the median and interquartile range. If the data was normally distributed, the mean sample differences were compared between the two

Table I. MRI scan parameters.

Parameters	T2WI	T1WI	T2FLAIR	3D ASL	DSC-PWI
TR (ms)	4,031	2,009.3	9,000	4,640	1,800
TE (ms)	105.2	24	95	10.7	30
TI (ms)	/	628	2475.9	/	/
Layers	18	18	18	36x2 <sup>a</sup>	20
Thickness (mm)	6.0	6.0	6.0	4.0	5
Layer space (mm)	1.5	1.5	1.5	/	1.5
Flip angle (°)	142	111	160	/	90
FOV (cm)	24x24	24x24	24x24	24x24	24x24
NEX	1.5	1.5	1.0	3	1
Matrix	416	256x256	256x256	/	128x128
Acquisition time (sec)	52	89	153	269	74

<sup>a</sup>36 images were labeled images, in which the blood water magnetization was inverted, and 36 were control images, in which the blood water magnetization was not inverted. TR, repetition time; TE, echo time; TI, inversion time; FOV, field of view; NEX, number of excitation; T2WI, T2 weighted imaging; T1WI, T1 weighted imaging; T2FLAIR, T2 fluid-attenuated inversion recovery; 3D ASL, three-dimensional arterial spin labeling; DSC-PWI, dynamic susceptibility contrast perfusion-weighted imaging.

groups using two-sample t-tests or Wilcoxon signed-rank tests. To analyze each parameter value and the relative differences in parameters in different grades of glioma Spearman's rank correlation analysis was used.  $P < 0.05$  was considered to indicate a statistically significant difference. Spearman's rank correlation analysis was performed to calculate the correlation between ASL-rCBF, DSC-rCBF and DSC-rCBV and pathological diagnosis of glioma grade. In the resulting correlation graphs, the difference in areas under the receiver operating characteristic (ROC) curves (i.e. the different diagnostic performance of the two tests) were calculated using Z tests, in order to identify the test with the best diagnostic value.

## Results

**Clinical data.** Glioma was pathologically confirmed in 50 patients. These were classified into high-grade and low-grade gliomas, according to WHO classification criteria (2007). There were 27 cases of LGGs, including 5 cases of ganglioglioma in GI, 4 cases of pilocytic astrocytoma in GI, 3 cases of obesity cell astrocytoma in GI and 15 cases of astrocytoma in GII. There were 23 cases of HGGs, including 3 cases of anaplastic oligodendroglioma in GIII, 9 cases of anaplastic astrocytoma in GIII and 11 cases of glioblastoma in GIV.

**Image information.** ASL-rCBF, DSC-rCBF and DSC-rCBV were measured in different grades of glioma by two radiologists. All the values were tested for consistency using the correlation coefficient for each parameter, and intraclass correlation values were obtained as  $> 0.90$ , in agreement between the two surveyors.

In 3D ASL and DSC-PWI pseudo-color images, LGGs demonstrated slightly high or low perfusion (determined subjectively by the authors; Fig. 1), while HGGs exhibited notably high perfusion. Furthermore, within the HGGs, tumors demonstrated uneven perfusion (Fig. 2).

**Correlation analysis between 3D ASL and DSC-PWI.** Spearman correlation analysis results demonstrated that ASL-rCBF had a significantly positive correlation with DSC-rCBF ( $r = 0.580$ ,  $P < 0.01$ ). In addition, ASL-rCBF had a significantly moderate positive correlation with DSC-rCBV ( $r = 0.431$ ,  $P < 0.01$ ).

**Correlation analysis between 3D ASL and DSC-PWI and pathology.** Spearman's rank correlation analysis was applied between ASL-rCBF, DSC-rCBF and DSC-rCBV of 3D ASL, DSC-PWI and pathological grade. The results showed a significant positive correlation between the values from ASL-rCBF, DSC-rCBF and DSC-rCBV and pathological grade ( $P < 0.01$ ; Table II), and the correlation coefficients were 0.487, 0.335 and 0.331, respectively. ASL-rCBF demonstrated the closest correlation with the pathological grade (Table III).

**3D ASL and DSC-PWI.** The parameter values of ASL-rCBF, DSC-rCBF and DSC-rCBV of the two types of perfusion (3D ASL and DSC-PWI) were used to produce the ROC curve (Fig. 3), which was then used to rate the diagnostic performance of 3D ASL and DSC-PWI in regards to HGGs. The results of the present study show that ASL-rCBF had the largest area under the ROC curve (0.836). The difference in areas under the ROC curve between DSC-rCBF, DSC-rCBV, DSC-rCBF and ASL-rCBF were analyzed using Z tests, showing that ASL-rCBF had the largest area under the ROC, but this not significantly different to DSC-rCBV and ASL-rCBF. When the cutoffs for ASL-rCBF, DSC-rCBF and DSC-rCBV were taken (2.24, 1.85 and 1.68), the sensitivities of HGG diagnosis were 83.2, 91.3 and 91.3%, and the specificities were 77.7, 63.9 and 66.7%, respectively (Table IV). The area under the ROC curve representing the difference between the three parameters of ASL-rCBF, DSC-rCBF and DSC-rCBV was not notable ( $P > 0.05$ ; Table V).

Table II. Comparison of low-grade gliomas with high-grade gliomas.

Parameter	Low-grade gliomas	High-grade gliomas	Z-test score	P-value
ASL-CBF, ml/100 g/min	50.64±35.89	88.03±37.16	-3.221	0.001
DSC-CBF, ml/100 g/min	15.15±15.85	41.08±37.88	-3.494	0.001
DSC-CBV, ml/100 g	3.12±3.71	8.40±6.07	-3.981	<0.01
ASL-rCBF	2.13±2.16	5.41±3.74	-4.06	<0.01
DSC-rCBF	3.79±5.31	8.26±7.46	-3.12	0.02
DSC-rCBV	3.94±5.81	9.84±10.93	-3.22	<0.01

ASL, arterial spin labeling; CBF, cerebral blood flow; DSC, dynamic susceptibility contrast; CBV, cerebral blood volume; rCBF, relative cerebral blood flow; rCBV, relative cerebral blood volume.

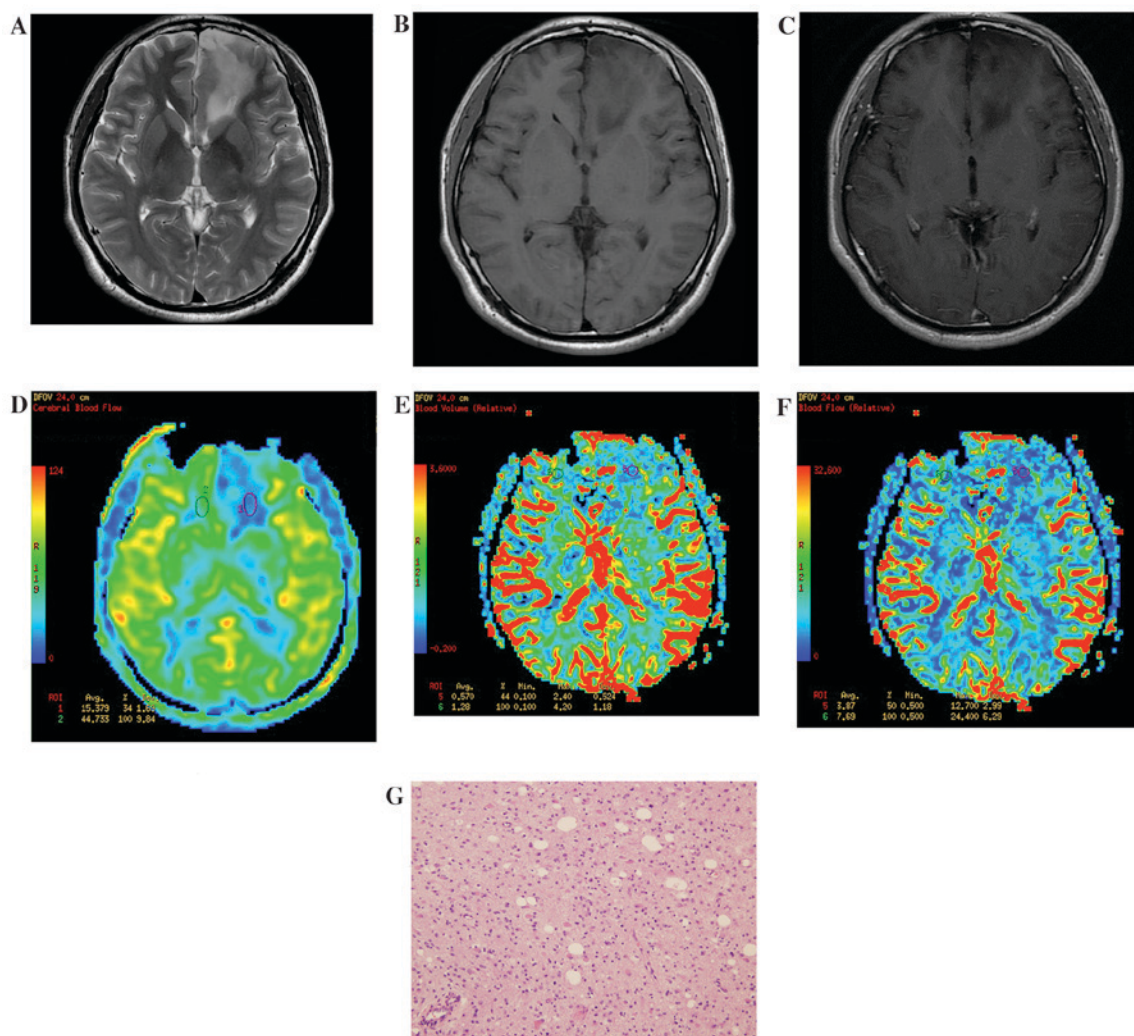


Figure 1. Results of imaging of a patient with a low-grade glioma located at the left side of the frontal lobe. (A) Routine T2WI. The focal lesion showed a slightly higher signal. (B) Routine T1WI. The focal lesion showed a slightly low signal. (C) Enhanced T1WI. The focal lesion had no obvious enhancement. (D) ASL-CBF imaging. Low perfusion of the tumor was observed, with a ASL-rCBF value of 0.46. (E) DSC-CBV imaging. Low perfusion of the tumor was observed, with a DSC-rCBV value of 0.44. (F) DSC-CBF imaging. Low perfusion of the tumor was observed, with a DSC-rCBF value of 0.5. (G) Hematoxylin and eosin staining of a low-grade glioma specimen (magnification, x40). The volume of tumor cells was large with abundant cytoplasm. WI, weighted imaging; ASL, arterial spin labelling; CBF, cerebral blood flow; DSC, dynamic susceptibility contrast; CBV, cerebral blood volume; r, relative.

## Discussion

Gliomas are rich in blood vessels and the vascular structures differ notably from normal vascular structure. Pathology

results show immature blood vessels in gliomas, with large cell gaps, incomplete basement membranes and lack of smooth muscle layers, resulting in higher permeability of these vessels (9,10). Angiogenesis levels are an important indicator

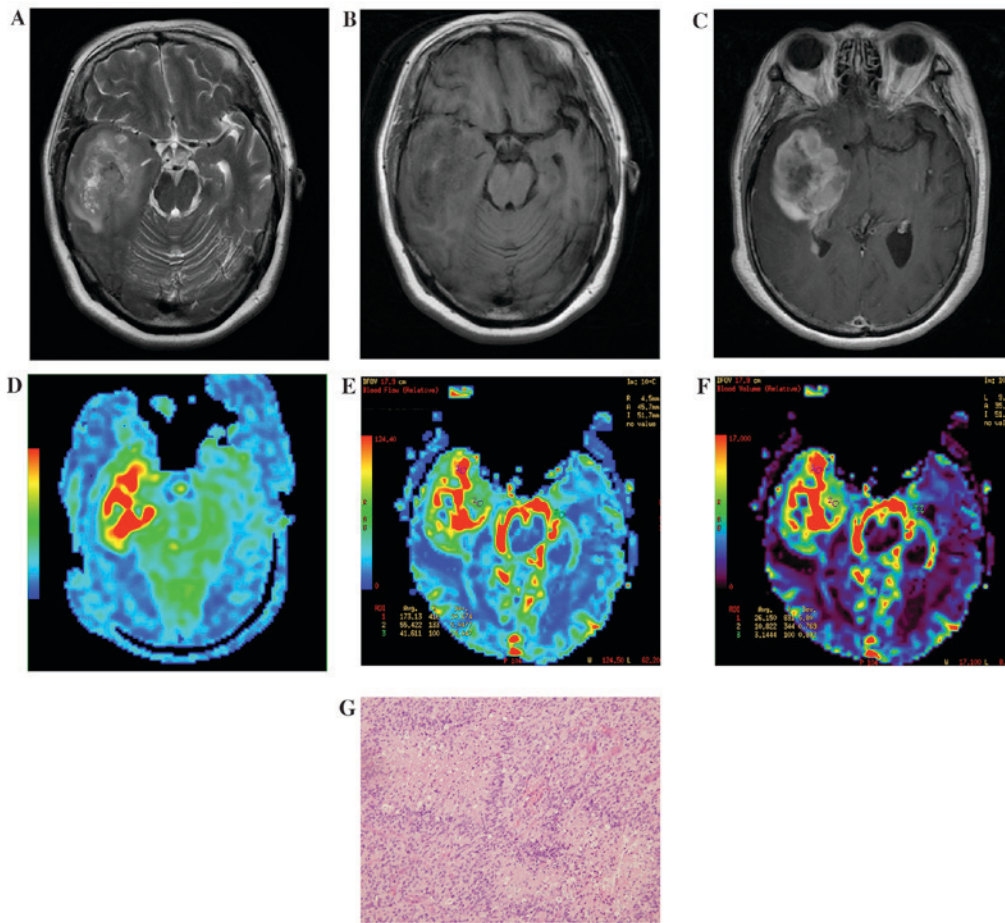


Figure 2. Results of imaging of a patient with a high-grade glioma located at the right side of the temporal lobe. (A) Routine T2WI. The mass showed a slightly higher and higher hybrid signal. The ring pool and saddle pool exhibited pressured narrowing. (B) Routine T1WI. The majority of the mass demonstrated uneven low signal mixed with high signal small patch sample bleeding. (C) Enhanced T1WI. The majority of the mass demonstrated **obvious uneven reinforcement** and the center area presented low signal without reinforcement. (D) ASL-CBF imaging. Visible and uneven high perfusion was observed, with a ASL-rCBF value of 8.03. (E) DSC-CBV imaging. The mass showed visible and uneven high perfusion, with a DSC-rCBV value of 8.16. (F) DSC-CBF imaging. The mass showed visible and uneven high perfusion, with a DSC-rCBF value of 4.16. (G) Hematoxylin and eosin staining of a high-grade glioma specimen (magnification, x40). Hyperplasia of the capillaries was observed and vascular endothelial cell enlargement and an increase number of vascular endothelial cells was evident. WI, weighted imaging; ASL, arterial spin labelling; CBF, cerebral blood flow; DSC, dynamic susceptibility contrast; CBV, cerebral blood volume; r, relative.

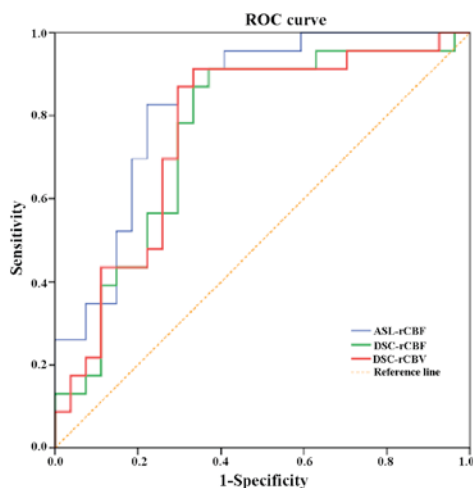


Figure 3. ROC curves of 3D ASL and dynamic susceptibility contrast perfusion-weighted imaging. 3D ASL relative cerebral blood flow had the largest area under the ROC curve, which was 0.836. ROC, receiver operating characteristic. 3D ASL, three-dimensional arterial spin labeling; rCBF, relative cerebral blood flow; DSC, dynamic susceptibility contrast perfusion-weighted imaging; rCBV, relative cerebral blood volume.

Table III. Correlation analysis between ASL-rCBF, DSC-rCBF and DSC-rCBV of 3D ASL, DSC-PWI and pathological grade.

Parameter	$r_s^a$	P-value
ASL-rCBF	0.487	<0.01
DSC-rCBF	0.335	<0.01
DSC-rCBV	0.331	<0.01

<sup>a</sup>Spearman's rank correlation analysis. ASL, arterial spin labeling; rCBF, relative cerebral blood flow; DSC, dynamic susceptibility contrast; rCBV, cerebral blood volume.

of glioma malignancy (11). The higher the grade of the glioma, the higher degree of vascular proliferation found.

MR perfusion imaging can quantitatively reflect tumor microvessel density, vascular nature and distribution, and can be used to assess the extent of brain tumor angiogenesis and invasion of the surrounding tissue (12). High levels of

Table IV. Comparison of the area under the ROC curve of the three parameters ASL-rCBF, DSC-rCBF and DSC-rCBV.

Indicators	Cutoff value	Area	Sensitivity (%)	Specificity (%)	Standard error	P-value
ASL-rCBF	2.24	0.836	83.2	77.7	0.057	<0.0001
DSC-rCBF	1.85	0.758	91.3	63.9	0.070	0.002
DSC-rCBV	1.68	0.767	91.3	66.7	0.070	0.001

ROC, receiver operating characteristic; ASL, arterial spin labeling; rCBF, relative cerebral blood flow; DSC, dynamic susceptibility contrast; rCBV, relative cerebral blood volume.

Table V. Comparison of the area under the ROC curve of three parameters (ASL-rCBF, DSC-rCBF and DSC-rCBV).

Indicators being compared	Estimate of the difference between the AUC	Standard error	95% confidence interval	$\chi^2$	P-value
DSC-rCBV vs. ASL-rCBF	-0.0569	0.0445	(-0.1441-0.0303)	1.6359	0.2009
DSC-rCBF vs. ASL-rCBF	-0.0681	0.0428	(-0.1519-0.0157)	2.5360	0.1113
DSC-rCBF vs. DSC-rCBV	0.0112	0.0131	(-0.0144-0.0369)	0.7342	0.3915

ROC, receiver operating characteristic; AUC, area under curve; DSC, dynamic susceptibility contrast; rCBV, relative cerebral blood volume; ASL, arterial spin labeling; rCBF, relative cerebral blood flow.

angiogenesis and corresponding blood flow are reflected in the perfusion imaging as an increase in the corresponding perfusion parameter values. In order to effectively extract this hemodynamic information, a diffusible tracer is injected which can travel within the vessels. Perfusion imaging can be divided into those that use an exogenous contrast agent and those that use an endogenous contrast. The former requires injection of paramagnetic contrast agents, such as gadolinium-diethylenetriamine pentaacetic acid, and includes DSC-PWI. The latter refers to the ASL technique.

DSC-PWI starts by rapid intravenous bolus injection of paramagnetic contrast agents. DSC-PWI has two methods, including SE-EPI and GRE-EPI. SE-EPI attains the T2-weighted contrast and T2\*-weighted contrast in GRE-EPI (13,14). When the contrast agent travels through nearby blood vessels, magnetic susceptibility differences between surrounding tissue can cause an uneven local magnetic field and accelerate protons to phase (a principle of DSC-PWI) in the process. Therefore, T2 or T2\* shortens, resulting in the signal of corresponding T2WI or T2\*WI decreasing transiently. According to the relationship between signal intensity changes (caused by contrast agents passing through the local brain tissue blood vessels) and time, a time-signal intensity curve is drawn. According to the curve, the relative value of the hemodynamic parameters can be obtained, and semi-quantitative study can be conducted by comparing the ratios of the contralateral site and ipsilateral site (15-17). For brain tumors, DSC-CBV is the most commonly used parameter, while the DSC-CBF is seldom used (18). In the present study, DSC-CBV and DSC-CBF parameters and their relative values are determined.

ASL imaging is a technique using an endogenous contrast agent, i.e. by using the spin labeling of water in arterial

blood (19). The initial application the 3D ASL in the present study demonstrated numerous clinical advantages compared with the DSC-PWI exogenous contrast perfusion. 3D ASL reflects perfusion and better reflects the nature of perfusion. Therefore, 3D ASL can accurately evaluate glioma micro-circulation information, reflecting the situation of tumor angiogenesis, and thus the glioma grade can more be accurately assessed. 3D ASL technology achieved 1,000 times of continuous mark in 1.5 sec, and thus overcame the shortcomings of traditional 2D ASL PASL, such as low signal:noise ratio and uneven perfusion effects in traditional pulse mark (20,21). So, 3D ASL can better evaluate glioma than DSC-PWI and evaluate a number of regions of the brain which cannot be evaluated by traditional 2D ASL, such as temporal regions, regions near the base of the skull and other regions close to gas structures (22,23).

Recently, numerous studies have shown that CBF values obtained from ASL have a high correlation with DSC-PWI CBF and CBV values through linear regression correlation analysis (24,25). Because there are individual differences in CBF value, in order to ensure accuracy of the quantitative measurement of CBF, the present study used a ratio of CBF values of white matter from the lesions side and the contralateral side as quantitative indicators to attain the relative CBF. Both MR perfusion imaging methods demonstrated that DSC-rCBF, DSC-rCBV and ASL-rCBF increase with glioma grade. The relative classification values were significantly positively correlated ( $P < 0.01$ ) with pathological grade, and the maximum parameter in the correlation coefficients was ASL-rCBF. The biggest area under the ROC curve was ASL-rCBF. The area under the ROV of DSC-rCBV was not statistically significant. ASL-rCBF, DSC-rCBF and DSC-rCBV were cutoff at 2.24,

1.85 and 1.68, the sensitivities of diagnosis of HGGs were 83.2, 91.3, and 91.3% and the specificities were 77.7, 63.9 and 66.7%, respectively. This illustrates that rCBF and rCBV can be good indicators of hemodynamic response in gliomas, and can be used to assess the pathological grade of glioma prior to surgery.

3D ASL perfusion imaging is non-invasive and does not require the injection of any exogenous contrast agent that may affect the physical, chemical and physiological properties of the blood. Therefore, 3D ASL retains the primitive physiological or pathological conditions to obtain hemodynamic parameters (19). The results of 3D ASL have high repeatability and good economic value. The present study demonstrated that ASL-rCBF had the largest area under the ROC curve, indicating that to some extent 3D ASL can replace the DSC-PWI, which may be useful in intracranial tumor studies when patients are allergic to exogenous contrast agents or have renal insufficiency (26-28). However, 3D ASL has a number of deficiencies compared with DSC-PWI. Firstly, 3D ASL has a relatively poor signal:noise ratio. Secondly, 3D ASL cannot measure as many parameters as DSC-PWI, and has only one CBF parameter, which limits its application. Nevertheless, 3D ASL is currently only in the initial stages of research, and it is believed that in the near future advances in this technology can overcome its shortcomings and make it widely applicable.

The present study had a number of limitations. Firstly, patients were collected in a short amount of time, the sample size was relatively small and measurement was somewhat biased (29,30). The potential for bias existed as if the head was tilted in the scan it would result in the marks on either side of the head not being at the same anatomic level and meaning the difference between the two sides would be inaccurate. Furthermore, the location of the arterial marker and the delay time are subjective and affected by human choice. Secondly, 3D ASL scanning time is relatively long, and is not conducive to patient examination. In the future, the sample size will be increased and classification of the grading of glioma further refined in order to meet WHO grading standards.

In conclusion, the present study demonstrated that 3D ASL and DSC-PWI perfusion imaging may be used to research the flow of blood to the brain glioma, help with preoperative classification and to help formulate the correct surgical procedure. 3D ASL technology is a completely noninvasive, no contrast method of whole brain perfusion imaging. 3D ASL technology is able to be used on patients with renal insufficiency or bleeding, therefore increasing the clinical application of this technology.

## References

- Fuller GN and Scheithauer BW: The 2007 Revised World Health Organization (WHO) Classification of Tumours of the Central Nervous System: Newly codified entities. *Brain pathology* 17: 304-307, 2007.
- Louis DN, Ohgaki H, Wiestler OD, Cavenee WK, Burger PC, Jouvet A, Scheithauer BW and Kleihues P: The 2007 WHO classification of tumours of the central nervous system. *Acta neuropathologica* 114: 97-109, 2007.
- Brat DJ, Parisi JE, Kleinschmidt-DeMasters BK, Yachnis AT, Montine TJ, Boyer PJ, Powell SZ, Prayson RA and McLendon RE: Neuropathology Committee, College of American Pathologists: Surgical neuropathology update: A review of changes introduced by the WHO classification of tumours of the central nervous system, 4th edition. *Arch Pathol Lab Med* 132: 993-1007, 2008.
- Sulman EP, Guerrero M and Aldape K: Beyond grade: Molecular pathology of malignant gliomas. *Semin Radiat Oncol* 19: 142-149, 2009.
- Gupta RK, Awasthi R, Rathore RK, Verma A, Sahoo P, Paliwal VK, Prasad KN, Pandey CM and Narayana PA: Under-standing epileptogenesis in calcified neurocysticercosis with perfusion MRI. *Neurology* 78: 618-625, 2012.
- Petersen ET, Zimine L, Ho YC and Golay X: Non-invasive measurement of perfusion: A critical review of arterial spin labeling techniques. *Br J Radiol* 79: 688-701, 2006.
- van den Bent MJ, Carpentier AF, Brandes AA, Sanson M, Taphoorn MJ, Bernsen HJ, Frenay M, Tijssen CC, Grisold W, Sipos L, *et al*: Adjuvant procarbazine, lomustine, and vincristine improves progression-free survival but not overall survival in newly diagnosed anaplastic oligodendrogliomas and oligoastrocytomas: A randomized European organisation for research and treatment of cancer phase III trial. *J Clin Oncol* 24: 2715-2722, 2006.
- Lehmann P, Monet P, de Marco G, Saliou G, Perrin M, Stoquart-Elsankari S, Bruniau A and Vallée JN: A comparative study of perfusion measurement in brain tumors at 3 Tesla MR: Arterial spin labeling versus dynamic susceptibility contrast-enhanced MRI. *Eur Neurol* 64: 21-26, 2010.
- Miller CR, Dunham CP, Scheithauer BW and Perry A: Significance of necrosis in grading of oligodendroglial neoplasms: A clinicopathologic and genetic study of newly diagnosed high-grade gliomas. *J Clin Oncol* 24: 5419-5426, 2006.
- Smith SF, Simpson JM, Brewer JA, Sekhon LH, Biggs MT, Cook RJ and Little NS: The presence of necrosis and/or micro-vascular proliferation does not influence survival of patients with anaplastic oligodendroglial tumours: Review of 98 patients. *J Neurooncol* 80: 75-82, 2006.
- Maia AC Jr, Malheiros SM, da Rocha AJ, da Silva CJ, Gabbai AA, Ferraz FA and Stávale JN: MR cerebral blood volume maps correlated with vascular endothelial growth factor expression and tumor grade in nonenhancing gliomas. *AJNR Am J Neuro-radiol* 26: 777-783, 2005.
- Covarrubias DJ, Rosen BR and Lev MH: Dynamic magnetic resonance perfusion imaging of brain tumors. *Oncologist* 9: 528-537, 2004.
- Zhao L, Fielden SW, Feng X, Wintermark M, Mugler JP III, Meyer CH: Rapid 3D dynamic arterial spin labeling with a sparse model-based image reconstruction. *Neuroimage* 121: 205-216, 2015.
- Chakravorty A, Steel T and Chaganti J: Accuracy of percentage of signal intensity recovery and relative cerebral blood volume derived from dynamic susceptibility-weighted, contrast-enhanced MRI in the preoperative diagnosis of cerebral tumours. *Neuroradiol J* 28: 574-583, 2015.
- Warmuth C, Gunther M and Zimmer C: Quantification of blood flow in brain tumors: Comparison of arterial spin labeling and dynamic susceptibility-weighted contrast-enhanced MR imaging. *Radiology* 228: 523-532, 2003.
- Petersen ET, Lim T and Golay X: Model-free arterial spin labeling quantification approach for perfusion MRI. *Magn Reson Med* 55: 219-232, 2006.
- Wang J, Alsop DC, Song HK, Maldjian JA, Tang K, Salvucci AE and Detre JA: Arterial transit time imaging with flow encoding arterial spin tagging (FEAST). *Magn Reson Med* 50: 599-607, 2003.
- Spampinato MV, Smith JK, Kwock L, Ewend M, Grimme JD, Camacho DL and Castillo M: Cerebral blood volume measurements and proton MR spectroscopy in grading of oligodendroglial tumors. *AJR Am J Roentgenol* 188: 204-212, 2007.
- Haller S, Zaharchuk G, Thomas DL, Lovblad KO, Barkhof F and Golay X: Arterial spin labeling perfusion of the brain: Emerging clinical applications. *Radiology* 281: 337-356, 2016.
- Steketee RM, Mutsaerts HJ, Bron EE, van Osch MJ, Majoie CB, van der Lugt A, Nederveen AJ and Smits M: Quantitative functional arterial spin labeling (FASL) MRI-sensitivity and reproducibility of regional CBF changes using pseudo-continuous ASL product sequences. *PLoS One* 10: e0132929, 2015.
- Hirai T, Kitajima M, Nakamura H, Okuda T, Sasao A, Shigematsu Y, Utsunomiya D, Oda S, Uetani H, Morioka M and Yamashita Y: Quantitative blood flow measurements in gliomas using arterial spin-labeling at 3T: Intermodality agreement and inter- and intraobserver reproducibility study. *AJNR Am J Neuroradiol* 32: 2073-2079, 2011.
- Dai W, Garcia D, De Bazelaire C and Alsop DC: Continuous flow-driven inversion for arterial spin labeling using pulsed radio frequency and gradient fields. *Magn Reson Med* 60: 1488-1497, 2008.
- van Gelderen P, De Zwart JA and Duyn JH: Pitfalls of MRI measurement of white matter perfusion based on arterial spin labeling. *Magn Reson Med* 59: 788-795, 2008.

24. Bisdas S, Kirkpatrick M, Giqlio P, Welsh C, Spampinato MV and Rumboldt Z: Cerebral blood volume measurements by perfusion-weighted MR imaging in gliomas: Ready for prime time in predicting short-term outcome and recurrent disease. *AJNR Am J Neuroradiol* 30: 681-688, 2009.
25. Zhang SX, Yao YH, Zhang S, Zhu WJ, Tang XY, Qin YY, Zhao LY, Liu CX and Zhu WZ: Comparative study of DSC-PWI and 3D-ASL in ischemic stroke patients. *J Huazhong Univ Sci Technolog Med Sci* 35: 923-927, 2015.
26. Sugahara T, Korogi Y, Kochi M, Ushio Y and Takahashi M: Perfusion sensitive MR imaging of gliomas: Comparison between gradient-echo and spin-echo echo-planar imaging techniques. *AJNR Am J Neuroradiol* 22: 1306-1315, 2001.
27. Pelrella JR and Provenzale JM: MR perfusion imaging of the Brain: Techniques and applications. *AJR Am J Roentgenol* 175: 207-219, 2000.
28. Sener A, Graff BA, Orheim TE, Schellhorn T, Josefsen R, Gadmar ØB and Nakstad PH: Measurements of diagnostic examination performance and correlation analysis using microvascular leakage, cerebral blood volume and blood flow derived from 3T dynamic susceptibility-weighted contrast-enhanced perfusion MR imaging in glial tumor grading. *Neuroradiology* 53: 435-447, 2011.
29. Amukotuwa SA, Yu C and Zaharchuk G: 3D Pseudocontinuous arterial spin labeling in routine clinical practice: A review of clinically significant artifacts. *J Magn Reson Imaging* 43: 11-27, 2016.
30. Yujie Qiu, Borogovac A, Laine A, Hirsch J and Asllani I: Tissue specific arterial spin labeling fMRI: A superior method for imaging cerebral blood flow in aging and disease. *Conf Proc IEEE Eng Med Biol Soc* 2014: 6687-6690, 2014.